Distribution Agreement

In presenting this thesis as a partial fulfillment of the requirements for a degree from Emory University, I hereby grant to Emory University and its agents the non-exclusive license to archive, make accessible, and display my thesis in whole or in part in all forms of media, now or hereafter now, including display on the World Wide Web. I understand that I may select some access restrictions as part of the online submission of this thesis. I retain all ownership rights to the copyright of the thesis. I also retain the right to use in future works (such as articles or books) all or part of this thesis.

Haoran Cheng Apr 4th , 2022

Estimating short- and long-term impact of COVID-19 on air quality, human health, and economic losses in China through machine learning counterfactual simulations

by

Haoran Cheng

Eri Saikawa
Adviser

Department of Environmental Sciences

Eri Saikawa

Adviser

Yang Liu

Committee Member

Seunghwa Rho

Committee Member

2022

Estimating short- and long-term impact of COVID-19 on air quality, human health, and economic losses in China through machine learning counterfactual simulations

By

Haoran Cheng

Eri Saikawa

Adviser

An abstract of
a thesis submitted to the Faculty of Emory College of Arts and Sciences
of Emory University in partial fulfillment
of the requirements of the degree of
Bachelor of Science with Honors

Department of Environmental Sciences

2022

Abstract

Estimating short- and long-term impact of COVID-19 on air quality, human health, and economic losses in China through machine learning counterfactual simulations

By Haoran Cheng

The short-term reduction in air pollutant concentrations due to acute lock-down during COVID-19 has been widely studied but few have quantified the amount of reduction in pollutant concentrations due to COVID. Fewer studies have analyzed the long-term impact of COVID-19 on local air quality or studied their social impacts. Our study uses machine learning counterfactual simulations to analyze both the acute (~weeks) and chronic (~year) impacts of COVID-19 on air quality, human health, and the economy in China. We analyzed concentrations of six air pollutants ($PM_{2.5}$, PM_{10}, SO_2, NO_2, CO, O_3) in 39 major cities in China during and after COVID-19 lockdown (January 28th, 2020 to April 30th, 2021) and predicted the pollutant concentrations for each pollutant in a counterfactual scenario – with no "COVID-19" lockdown, using local meteorological data with XGBoost machine learning model. We calculated the associated health and economic impacts in the counterfactual world and compared them with the real-world impact. Among the cities surveyed, 64%, 93%, 82%, 95%, 81% of the cities showed a statistically significant reduction between the observed $PM_{2.5}$, PM_{10}, SO_2, NO_2, CO during the lockdown, compared to the model prediction. We observed an increase in O_3 concentrations in all cities during the lockdown but this increase was only significant for 34% of the cities analyzed. The total amount of observed gaseous oxidants (O_x= NO_2+O_3) remained mostly the same, compared to the counterfactual scenario. In both the observed and predicted simulations, NO_2 and O_3 were the leading cause of excess health and economic burdens. For the post-lockdown period, the observed concentrations of each pollutant were still lower than the counterfactual scenario for all regions combined but the differences were much smaller (more than 90% reduction in differences) compared to those during the lockdown period. The health and economic burdens due to air pollution continued to be lower with COVID than without in the post-lockdown period, except for O_3 in the Northeast (NE), Southeast (SE) and Southwest (SW) regions. The implementation of COVID lockdown in China resulted in a significant reduction of various air pollutant concentrations. Long-term impacts varied among the cities and pollutants studied. The chronic, post-lockdown impact of COVID-19 on China's air quality is yet to be determined and further research is needed.

Estimating short- and long-term impact of COVID-19 on air quality, human health, and economic losses in China through machine learning counterfactual simulations

By

Haoran Cheng

Eri Saikawa

Adviser

A thesis submitted to the Faculty of Emory College of Arts and Sciences
of Emory University in partial fulfillment
of the requirements of the degree of
Bachelor of Science with Honors

Department of Environmental Sciences

2022

Acknowledgements

I am sincerely grateful to Dr. Saikawa for her consistent guidance for me on this project. This project would not be possible at all without constant mentorship and encouragement from her.

I would also like to express my gratitude for our former postdoc Dr. Qiao Zhu and machine learning expert Dr. Tianlong Xu as they helped me familiarize with machine learning and assisted in creating the model used in the paper.

I appreciate the constructive feedback and comments from Dr. Yang Liu and Dr. Seunghwa Rho as they serve as my thesis committee members.

I'm thankful to my mom and dad for raising me and unconditionally supporting all my dreams to the best of their abilities for the past 22 years of my life.

Last but not least, I would like to especially thank my grandmother for making me who I am today. May she rest in peace and be very proud of what I have achieved.

Table of Contents

1 Introduction

In 2019, a new coronavirus was first reported and became known as severe acute respiratory syndrome coronavirus 2 (SARS-CoV-2). The disease was named coronavirus disease 2019 (COVID-19) and has been declared a pandemic by the World Health Organization, causing a large threat to public health. So far till 2022 March (or something that you have the data for), it has caused 470 million infections and 6.07 million deaths globally, becoming one of the new “Big Three” infectious diseases in history, together with Tuberculosis, Malaria, and HIV/AIDS (Makam et al., 2021). Economic losses associated with the prevention and treatment of COVID-19 as well as reduction in the working population due to infection are estimated to be 12.5 trillion dollars (Reuters, 2022). Given the health impacts caused by COVID-19, more than 140 countries implemented a wide range of strict non-pharmaceutical interventions after March 2020 to slow the infection rate, according to the Oxford COVID-19 Government Response Tracker (OxCGRT). These lockdown policies led to various social, economic, and environmental consequences on our day-to-day activities (Cole et al., 2020).

China was the first country to impose a city-level lockdown policy and a large wave of national lockdown lasted until the first half of 2020. As the result of the lockdown, there were significant short-term concentration reductions in several air pollutants ($PM_{2.5}$, PM_{10}, SO_2, NO_2, CO), as well as an increases in O_3 (Wang et al., 2020; Li et al., 2021; Chen et al., 2021). There were also considerable changes in associated premature mortality and health economic losses due to the lockdown (Nie et al., 2021). Multiple attempts have already been made to quantify the exact proportion of change due to COVID-19 using difference-in-difference analysis or machine learning counterfactual simulations (Hu et al., 2021; Bybarczyk et al., 2021; Lovric et al., 2021; He et al., 2020). However, such studies are usually based on only one or few cities. Also, many are focused only on the change in air quality, neglecting associated health or economic costs into account. What is more, past studies have suggested that the impact of COVID-19 on air quality is long lasting. In other words, even in places where COVID-19 is largely contained and there is no further nation-wide lock down, it is likely that these places will still remain under the chronic influence of COVID-19. However, few papers have investigated the air quality change in China in the year after COVID and even less research analyzes the economic and health impacts.

To help answer these questions, we created a counterfactual "COVID-19 free" scenario and predicted the concentration of various pollutants in that scenario using meteorological conditions from previous years. We then calculated the differences between the reality and the counterfactual to quantity the attributable fraction of change in air quality due to COVID-19. We further conducted a difference-in-difference analysis to estimate the changes in air quality after lockdown. Eventually, we estimated the combined excess health and economic burden for both the lockdown and the 1-year post-lockdown period.

2. Data and Method

2. 1 Data

2.1.1 Air Quality Data

AQICN (https://aqicn.org/) is the website of the World Air Quality Index project that includes air quality observational data from different monitoring stations around the world. It includes concentrations of six major air pollutant species, including $PM_{2.5}$, PM_{10}, SO_2, NO_2, CO and O_3 and has daily pollutant Air Quality Index (AQI) of all six species for major cities around the world. All AQIs were converted to raw concentrations in the following analyses, using the standard equation provided by the Environmental Protection Agency (EPA).

2.1.2 Meteorological Data

China meteorological data service center (http://data.cma.cn/en) is an upgraded system of the meteorological data sharing network. Its meteorological data archive ranges from surface meteorological monitoring stations, upper air meteorological stations, modeling predictions, radar reflectivity and satellite data. For this paper, average temperature, average relative humidity, minimal relative humidity, average wind speed, maximum wind speed, maximum wind speed wind direction, extreme wind speed, extreme windspeed direction, hours of daylight and precipitation per day for each city from surface meteorological stations are included.

2.1.3. Demographic Data

China National Statistical Yearbook is an annual statistical publication by National Bureau of Statistics of China that reflects comprehensively the economic and social development of China. The book is divided into 28 chapters and includes data, such as population, prices, people's livelihood and others. For our research purpose, we used the 2020 updated version and included baseline mortality rate, GDP per capita and CPI for each city. Data can be accessed online, using the following website: http://data.stats.gov.cn/easyquery.htm?cn=C01.

2.2 Method

2.2.1 Sample inclusion and grouping

We analyzed air quality in 39 cities in China, including all provincial capitals and other major cities (Table 1 and Figure 2). Pollutant concentrations, meteorological conditions, demographic information of all cities are included from 2017 January 1st to 2021 April 30th. The cities were then separated into eight spatial groups based on their geographical locations, including North (N), Northeast (NE), Northwest (NW), Southwest (SW), Southeast (SE), South (S), East (E), and Central (C).

Table 1. A list of 39 cities included in the analysis and their respective eight geographical regions

Regions	Cities
North (N)	Hohhot (HHT), Taiyuan (TY), Beijing (BJ), Tianjin (TJ), Baoding (BD), Shijiazhuang (SJZ)
Northeast (NE)	Harbin (HB), Changchun (CC), Shenyang (SY)
Northwest (NW)	Urumqi (URQ), Xining (XN), Lanzhou (LZ), Yinchuan (YC), Xian (XA)

Southwest (SW)	Lhasa (LS), Chengdu (CD), Kunming (KM), Guiyang (GY), Chongqing (CQ)
Southeast (SE)	Nanchang (NC), Fuzhou (FZ), Hangzhou (HZ)
South (S)	Nanning (NN), Haikou (HK), Guangzhou (GZ), Dongguan (DG), Shenzhen (SZ)
East (E)	Hefei (HF), Shanghai (SH), Suzhou (SZ), Nanjing (NJ), Wuxi (WX), Jinan (JN), Qingdao (QD), Weifang (WF)
Central (C)	Wuhan (WH), Changsha (CS), Zhoukou (ZK), Zhengzhou (ZZ)

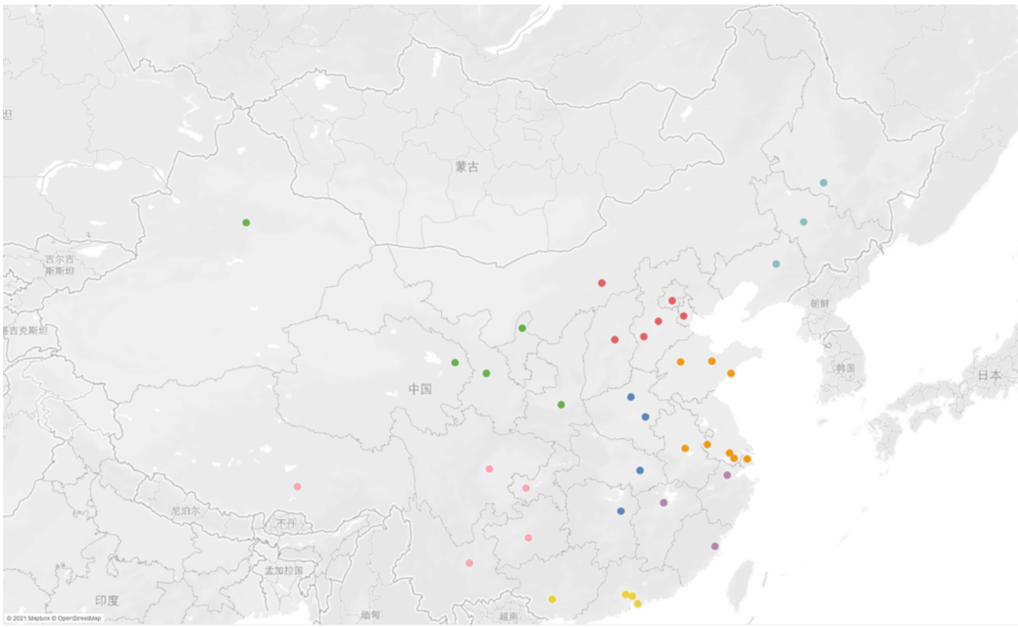

Figure 1. Cities studied in this work. Colors indicate the regions (pink—SW, yellow— S, purple—SE, blue—C, green—NW, orange—E, red—N, indigo—NE)

Data from each city was then further separated into groups based on seasonality and relations to the National lockdown: pre-lockdown, during lockdown, and post-lockdown. The lockdown period for each city was determined from the news (https://www.thepaper.cn/newsDetail_forward_7231201) and has been summarized in Table 2.

Table 2: Start and end date of lockdown for each individual province.

Province	Start Date	End Date
Anhui	2020/1/24	2020/3/15
Beijing	2020/1/24	2020/4/30
Chongqing	2020/1/24	2020/3/24
Fujian	2020/1/24	2020/2/26
Gansu	2020/1/25	2020/2/21
Guangdong	2020/1/23	2020/2/24
Guangxi	2020/1/24	2020/2/24
Guizhou	2020/1/25	2020/2/23
Hainan	2020/1/25	2020/2/26
Hebei	2020/1/25	2020/4/30
Heilongjiang	2020/1/25	2020/3/25
Henan	2020/1/25	2020/3/19
Hubei	2020/1/24	2020/5/2
Hunan	2020/1/23	2020/3/31
Jiangsu	2020/1/25	2020/3/27
Jiangxi	2020/1/24	2020/3/20
Jilin	2020/1/25	2020/3/20
Liaoning	2020/1/25	2020/2/22
Neimenggu	2020/1/25	2020/2/25
Ningxia	2020/1/25	2020/2/28
Qinghai	2020/1/25	2020/3/6
Shaanxi	2020/1/25	2020/2/28
Shandong	2020/1/24	2020/3/7
Shanghai	2020/1/24	2020/3/24
Shanxi	2020/1/25	2020/3/10
Sichuan	2020/1/24	2020/3/25
Tianjin	2020/1/24	2020/4/30
Xinjiang	2020/1/25	2020/3/21
Xizang	2020/1/29	2020/3/6
Yunnan	2020/1/24	2020/2/24
Zhejiang	2020/1/23	2020/3/23

2.2.2 Air Quality Change

We performed a counterfactual simulation using the Extreme Gradient Boosting (XGBoost) machine learning model in Python. XGBoost is an ensemble learning method that uses multiple learning algorithms at the same time to obtain better predictive performance than could be obtained from any of the constituent learning algorithms alone. XGBoost is a scalable, distributed gradient-boosted decision tree (GBDT) machine learning library that provides a parallel tree boosting and has become the leading machine learning library for regression, classification, and ranking problems. We included meteorological conditions as independent variables and different pollutant concentrations as dependent variables from 2017-2018 for each city in our training dataset. We then used grid search and cross-validation to choose the optimal set of hyperparameters values that minimize Mean Square Error (MSE) and the hyperparameters we tuned include maximum depth per tree, learning rate and number of trees in our ensemble. The model was developed and tuned by our former postdoc Dr. Qiao Zhu and data scientist Dr. Tianlong Xu and we used their model for the following analysis.

To evaluate the predictions of a model with observational data, we used the statistical performance parameters used in Hanna et al. (1993), which have been widely used in air quality performance evaluation (Chang et al., 2004). These parameters include fractional bias (FB), geometric mean bias (MG), normalized mean square error (NMSE), geometric variance (VG), correlation coefficient (R), and the fraction of predictions within a factor of two of observations (FAC2):

$$\mathrm{FB} = \frac{\left(\overline{\mathrm{C_o}} - \overline{\mathrm{C_p}}\right)}{0.5\left(\overline{\mathrm{C_o}} + \overline{\mathrm{C_p}}\right)}$$

$$\mathrm{MG} = \mathrm{e}^{\left(\overline{\ln \mathrm{C_o}} - \overline{\ln \mathrm{C_p}}\right)}$$

$$\mathrm{NMSE} = \frac{\overline{\left(\mathrm{C_o} - \mathrm{C_p}\right)^2}}{\overline{\mathrm{C_o}}\,\overline{\mathrm{C_p}}}$$

$$\mathrm{VG} = \mathrm{e}^{\overline{\left[(\ln \mathrm{C_o} - \ln \mathrm{C_p})^2\right]}}$$

$$\mathrm{R} = \frac{\overline{(\mathrm{C_o} - \overline{\mathrm{C_o}})(\mathrm{C_p} - \overline{\mathrm{C_p}})}}{\sigma \mathrm{C_p} \sigma \mathrm{C_o}}$$

$$FAC2 = fraction\ of\ data\ that\ satisfies\ 0.5 \le \frac{C_p}{C_o} \le 2.0$$

Where C_p is model prediction, Co is observation, and the bar indicates the average over the variable and σC is the standard deviation over the dataset. A perfect model would have MG, VG, R, and FAC2 = 1.0; and FB and NMSE = 0. Note that since FB and MG measure only the systematic bias of a model, it is possible for a model to have predictions completely out of phase of observations and still have FB = 0 or MG = 1.0 because of canceling errors.

We then used the model to predict the air quality in 2020 and 2021 in a counterfactual world where there was no COVID-19. We calculated the difference between the observed and the simulated as the magnitude of reduction due to COVID-19. Nonparametric Wilcoxon tests were performed to test the level of statistical significance for differences as followed, due to non-normally distributed data.

$$z = \frac{W_s - \frac{n(n+1)}{4}}{\sqrt{\frac{n(n+1)(2n+1)}{24}}}$$

Where n is the number of pairs where difference is not 0 and w_s is the smallest of absolute values of the sums.

2.2.3 Health Impact Analysis

Health and Economic impact analyses are conducted to look into the long-term impact of COVID-19. The estimated health burden owing to short-term exposure to air pollutants can be calculated as follows (Silva et al. 2013):

$$M = \sum_{1}^{n} AF_i \times BM$$

$$AF_i = \frac{RR_i - 1}{RR_i}$$

$$RR_i = e^{(\beta \times (C - C_0))}$$

Where M denotes the total mortality from air pollution, n is the total number of days, BM is the daily baseline mortality, AFi is the daily attributable fraction associated with short-term exposure to an air pollutant i. In Eq. (2), RRi is the daily relative risk associated with short-term exposure to an air pollutant i. In Eq. (3), β is the concentration-response coefficient for health endpoints due to an exposure to air pollutants, which were obtained from recent epidemiological studies (Shang et al.2013) (Table 3); Ci is the daily concentration of an air pollutant i; Ci0 is the daily threshold concentration of air pollutants, which is assumed to be zero here, as in previous studies (Chen et al. 2017; Yao et al. 2020).

Table 3: Response coefficient (β) for each pollutant species

Pollutant species	Response Coefficient (β/%)
$PM_{2.5}$ (10 μg/m³)	0.38
PM_{10} (10 μg/m³)	0.32
SO_2 (10 μg/m³)	0.81
NO_2 (10 μg/m³)	1.30
CO (1 mg/m³)	3.70
O_3 (10 μg/m³)	0.48

2.2.4 Economic Impact Analysis

The value of statistical life (VSL) method was applied to estimate the economic loss due to mortality caused by short-term exposure to air pollution. The associated health economic loss (HEL) was calculated by:

$$HEL = M \times VSL_{k,2019}$$

Where M is the health burden calculated from Eq. (1). $VSL_{k,2019}$ is the adjusted VSL in city k in 2019 and can be calculated by Eq. (5) (Yao et al. 2020; Zhao et al. 2016):

$$VSL_{k,2019} = VSL_{b,2010} \times (\frac{G_{k,2010}}{G_{2010}})^{\delta} \times \ (1 + \%\Delta P_k + \%\Delta \gamma_k)^{\delta}$$

Where $VSL_{b,2010}$ is the base value of VSL in Beijing in 2010 (1.68 million RMB). $G_{k,2010}$ is the GDP (gross domestic product) per capita in city k in 2010. G_{2010} is the GDP per capita in Beijing in 2010. δ is the income elasticity, which is assumed to be 0.8 recommended by the Organization for Economic Co-operation and Development (OECD) (OECD, 2014). %Δ Pk represents the price inflation, i.e. percentage change in CPI (consumer price index) from 2010 to 2019; %Δγk is the post-2010 income growth, i.e. the percentage change of GDP per capital in city k from 2010 to 2019. The CPI and GDP data of each city are available from the China Statistical Yearbook 2019 (http://data.stats.gov.cn/easyquery.htm?cn=C01). Figure 2 is the overall flowchart of our study design, concerning how we split the data, train the model and calculated the associated health and economic impact.

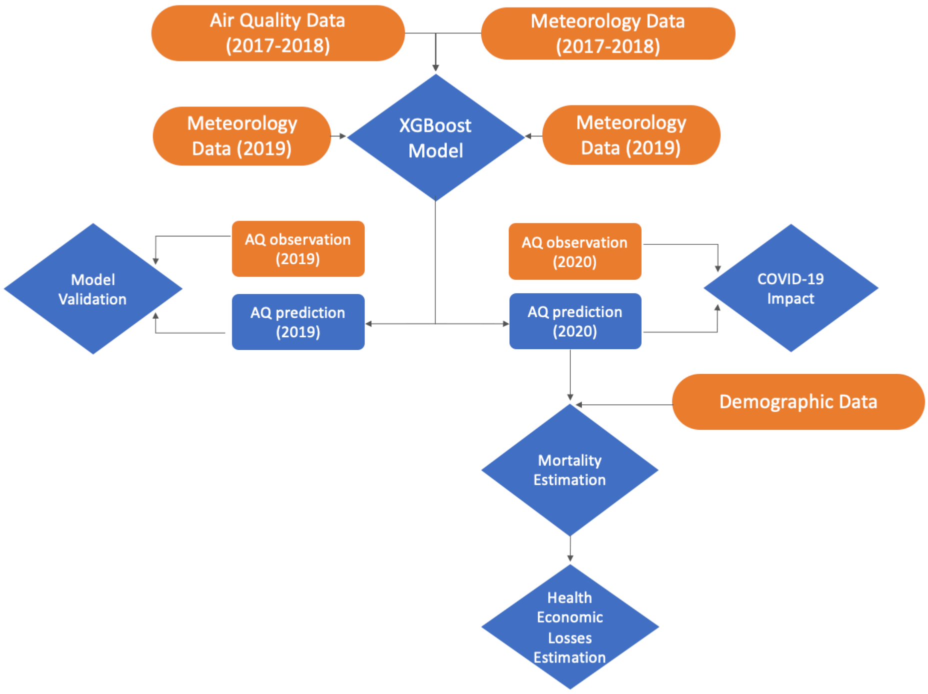

Figure 2. A flowchart illustrating how we built and validated our model before using the model output for health and economic analyses.

3 Results

3.1 Model Validation using 2019 observational data

The model validation part was done by Dr. Qiao Zhu. Figure 3 summarizes the most important ten predictors in our model based on training dataset, seven of which are dummy variables for seasons and months. The baseline value for year, season and month dummy are 2018, fall, and January. The most important dummy variable is season_spring and the most important non-dummy variable is average temperature. The figure is scaled so that the importance of season_spring in predicting the output is 1 and importance of other predictors is relative to season_spring.

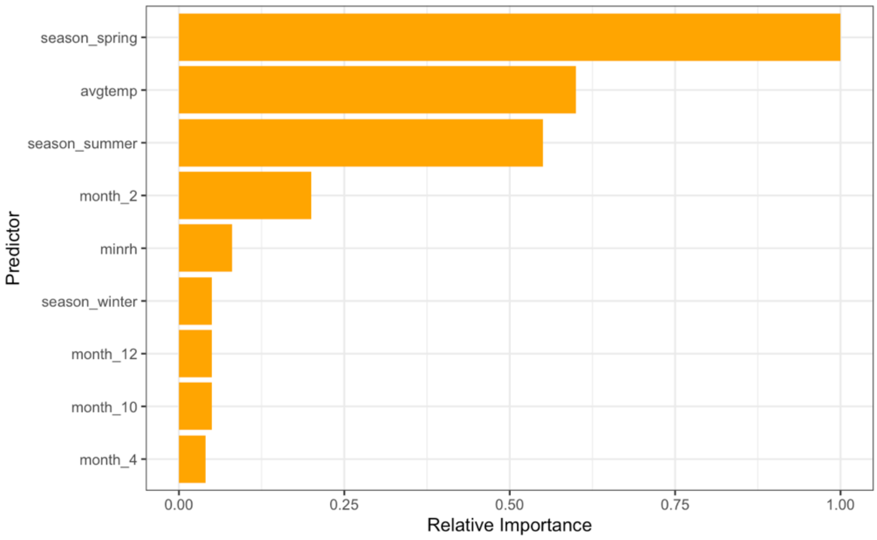

Figure 3: The most importance 10 predictors in the XGBoost model and their relative importance to the most important predictor (season_spring) (Figure Courtesy: Dr. Qiao Zhu).

Table 4 summarizes the parameters we calculated to evaluate model performance. Theoretically, a perfect model would have geometric mean bias (MG), geometric variance (VG), correlation coefficient(R), and fraction of predictions within a factor of two of observations (FAC2) = 1.0; and FB (Fractional Bias) and NMSE (Normalized Mean Square Error) = 0.0. For our data, the model has FB lower than 10%, high MG above 0.95, low NMSE less than 0.01, high R over 0.7, and high FAC2 over 86%, for all species other than for SO_2. The reason why the model performs relatively poorer for SO_2 is most likely caused by its low concentrations. The fractions of differences between observations and prediction are larger when absolute values are low compared to when them are high. Overall, the model does a good job of predicting pollutant concentrations pre-COVID and gives us enough confidence in estimating air quality, using the meteorological data.

Table 4: Evaluation Table for the XGBoost model using 2019 as test data. FB = Fractional Bias, MG = Geometric Mean Bias, NMSE = Normalized Mean Square Error, VG = Geometric Variance, R = correlation coefficient, FAC2 = fraction of observation within a factor of 2 of the observations

Species	FB	MG	NMSE	VG	R	FAC2
$PM_{2.5}$	-0.029	0.96	1.80e-03	1.42	0.74	0.86
PM_{10}	-0.068	0.95	6.99e-04	1.41	0.80	0.86
SO_2	-0.240	0.88	5.40e-02	1.39	0.79	0.76
NO_2	-0.049	0.96	4.40e-03	1.35	0.75	0.93
CO	-0.060	0.96	2.21e-05	1.35	0.72	0.93
O_3	0.026	0.99	1.30e-03	1.40	0.79	0.89

3.2 Comparison of simulation and observational data during lockdown

3.2.1 Air Quality Change

During lockdown, many regions exhibited statistically significant differences between observed and simulated concentrations for $PM_{2.5}$, PM_{10}, SO_2, NO_2, and CO (Figure 4). To be specific, the differences between observations and simulations were statistically significant for all the five species according to Wilcoxon test for N, NW, SE, S, E, C. On a city level, 64%, 93%, 82%, 95%, and 81% of the cities surveyed showed a statistically significant reduction in $PM_{2.5}$, PM_{10}, SO_2, NO_2, and CO concentrations, respectively, due to COVID lockdown, according to the Wilcoxon test. The percentage reductions due to COVID were 17%, 26%, 24%, 36%, 24% for $PM_{2.5}$, PM_{10}, SO_2, NO_2, and CO concentrations, respectively. On a regional level, the differences were statistically significant for all eight regions for PM_{10}, NO_2 and CO. For $PM_{2.5}$, the differences were significant for all regions other than NE and for SO_2, the differences were significant for all regions other than SW.

The lockdown has impacted O_3 differently than the other air pollutants. O_3

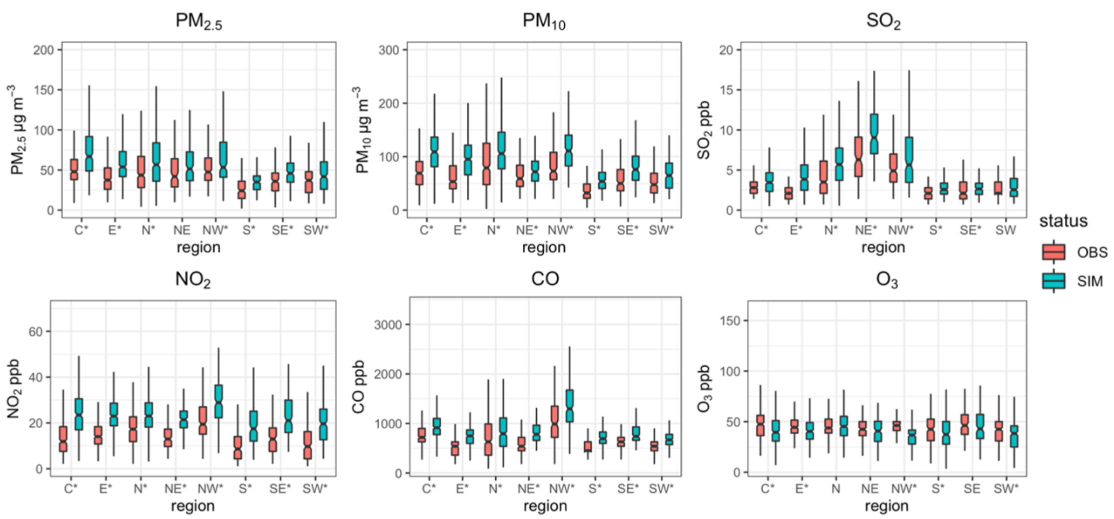

concentrations were higher during the COVID lockdown. The O_3 concentrations during the lockdown were 11% greater than the values simulated without COVID and the increase was found in 34 cities in 8 regions. However, the Wilcoxon test indicated that this increase was not statistically significant for most of the cities. At the regional level, five (C, E, NW, S, SW) out of eight regions had significant differences for O_3. At the city level, the increase was only significant for 34% of cities (16 out of 35) surveyed.

Figure 4. Observed pollutant concentration in 2020 during lockdown period compared against those in a counterfactual simulation without COVID-19. * symbol next to the region abbreviation on the X-axis illustrates regions with significant differences between the observed and the predicted using Wilcoxon tests.

Table 5 summarizes the same six parameters that we use to validate model performance during the lockdown period. Compared to 2019 where absolute FB is less than 0.1 for all pollutants other than SO_2, the FB for during lockdown period is larger than 0.1 for all speies, and aboslute FB for NO_2 in particularly is more than 0.4. This is also consistent with our findings that decrease in NO_2 concentration is the most significant during lockdown. MG and FAC2 are both less than 0.9 for $PM_{2.5}$, PM_{10}, SO_2, NO_2 and CO.

Table 5: Evaluation Table for the XGBoost model by comparing 2020 simulation data with observational data

Species	FB	MG	NMSE	VG	R	FAC2
$PM_{2.5}$	-0.187	0.89	1.26e-03	1.38	0.72	0.79
PM_{10}	-0.305	0.85	6.90e-04	1.38	0.63	0.73
SO_2	-0.276	0.87	5.60e-02	1.41	0.83	0.75
NO_2	-0.433	0.79	5.40e-03	1.33	0.65	0.64
CO	-0.234	0.88	2.09e-05	1.33	0.77	0.85
O_3	0.105	1.06	1.70e-03	1.43	0.58	0.91

3.2.2 Premature Mortality

Tables 5 and 6 describe the excess mortality during the lockdown by region and by species. Excess mortalities due to exposure to SO_2, CO, and NO_2 are higher in the observed compared to simulated values for all regions. NO_2 is the primary contributor to excess mortality in counterfactual simulations both nationally and for each region individually. In reality, however, O_3 is the primary contributor to excess mortality for seven out of the eight regions (except for NW, where NO_2 is still the primary health concern in observation) and in aggregate nationally. The nationwide avoided excess mortality due to NO_2 is the greatest among all pollutant species (3.83 people per million people per day, later all same unit unless otherwise stated). All regions experienced an increase in O_3 associated excess mortality and the mortality was higher in the east and north in general (C, E, NE, N) compared to the South and West (S, SW). The increase is biggest for NW (1.82) and smallest for N (0.37). This is also consistent with findings in earlier studies that short-term excess mortality is more attributable to NO_2 and $O_{3.}$ (Yao et al., 2020; Nie et al., 2021; Xiao et al., 2021) Even though the raw concentration of NO_2 is less than that $PM_{2.5}$, it still causes many more deaths in the short-term, due to a much larger exposure response coefficient which is obtained from and confirmed by previous meta-analysis (CITATION).

Nationally-combined CO mortality followed next (4.92), with a similar impact due to PM_{10} (4.62). It is also interesting to notice that among all regions, CO-associated excess death was still the highest in Central (where Wuhan is) in observation. SO_2 caused the least excess mortality, both in observation and simulations for each region separately. Regionally speaking, in the modeled result, Central has the greatest combined mortality due to air pollution (42.08). South has the lowest combined mortality (21.86). In reality, Northeast has the greatest combined mortality (33.78) and South has the lowest combined mortality (16.09). The combined observation-simulation difference is greatest for East (-10.43) and smallest for Northeast (-4.78)

Table 6: Excess mortality by species during lockdown (death per million people per day)

Species	Obs	Est	Diff
$PM_{2.5}$	2.84	3.35	-0.52
PM_{10}	4.62	6.17	-1.56
SO_2	1.45	1.85	-0.4
NO_2	6.52	10.35	-3.83
CO	4.92	6.3	-1.39
O_3	7.55	6.68	0.87

Table 7: Excess mortality by regions during lockdown (death per million people per day)

Region	Obs	Est	Diff
NE	33.78	38.56	-4.77
N	29.00	34.48	-5.48
NW	31.89	37.55	-5.66
SW	26.55	32.28	-5.74
S	16.09	21.86	-5.76
SE	23.65	30.13	-6.49
C	31.78	42.08	-10.30
E	30.28	40.71	-10.43

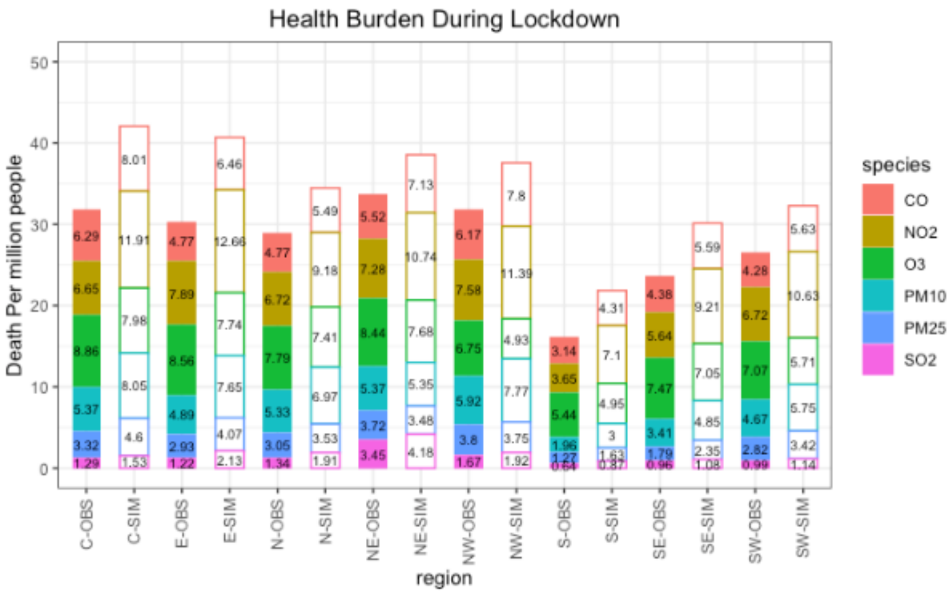

Figure 5. Observed excess mortality per species (death per million people) in 2020 during lockdown period compared against those in a counterfactual simulation without COVID-19.

3.2.3 Health Economic Losses

The distribution of health economic losses is overall similar to that of excess mortality. O_3 is the pollutant with the greatest economic burden for six out of the eight regions during the lockdown, with the exception of E & NW, where NO_2 was the primary Economic concern. O_3 caused the greatest economic losses in the east and north regions (NE, N, SE) and also resulted in additional economic losses during the lockdown, compared to the counterfactual simulation for all regions. The excess losses were the greatest for NW (2.45 million yuan per million people per day, following all the same unit unless otherwise stated) and smallest for N (0.70). Due to the large concentration reduction found for NO_2 during the lockdown, we found that substantial economic loss (6.53 million yuan per million people per day) was avoided due to the COVID lockdown.

Table 8: Health Economic Losses by species during lockdown (million yuan per million people per day)

Species	Obs	Est	Diff
$PM_{2.5}$	4.70	5.67	-0.98
PM_{10}	7.70	10.49	-2.80
SO_2	2.30	3.01	-0.71
NO_2	11.05	17.58	-6.53
CO	8.49	10.88	-2.39
O_3	12.49	11.13	1.35

Table 9: Health Economic Losses by regions during lockdown (million yuan per million people per day)

Region	Obs	Est	Diff
NE	42.71	48.75	-6.04
NW	42.82	50.42	-7.60
SW	38.61	46.95	-8.34
S	28.14	38.21	-10.08
N	56.84	67.65	-10.81
SE	45.98	58.71	-12.74
C	49.48	65.52	-16.04
E	69.14	93.88	-24.74

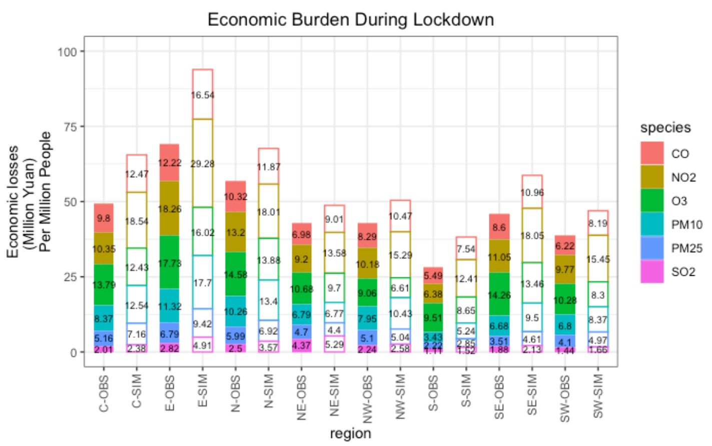

Figure 6. Observed excess health economic losses per species (million yuan per million people) in 2020 during lockdown period compared against those in a counterfactual simulation without COVID-19.

3.3 Comparison of simulation and observational data post lockdown

3.3.1 Excess mortality

The difference between observation and counterfactual simulations is smaller after the lockdown. The difference between the combined health burden calculated from the machine learning simulation result and that from actual observation is -0.28 people per million people per day after lockdown, compared to -1.14 people per million people per day during the lockdown. To be specific, the difference for $PM_{2.5}$, PM_{10}, SO_2, NO_2, CO, and O_3 were -0.52, -1.56, -0.4, -3.83, -1.39, and 0.87 during the lockdown and -0.13, -0.03, -0.19, -0.8, -0.57 and 0.03 after lockdown, respectively. The mortality due to the exposure to SO_2, NO_2, CO by region were lower during COVID compared to counterfactuals for all regions. Among all species, the COVID impact was found to be the greatest for NO_2. In the counterfactual scenario, NO_2 is the leading health concern for six out of eight areas but using the observed values, NO_2 only results in the largest health impacts in four areas (E, NE, NW, SW), while O_3 is important in the remaining four regions (C, N, S, SE). Geographically, O_3-associated economic losses were higher in the east and north in general (C, E, NE, N), compared to south and west (S, SW, SW). SO_2 was still the pollutant with the least health burden.

In spite of the significant reduction in excess mortality, the total gaseous oxidants (O_x=O_3+NO_2) remained mostly unchanged. Table 10 summarizes the total gaseous oxidants before lockdown and reduction were much smaller compared to changes in NO_2 and O_3 only. Earlier studies also yielded similar results (Shi, et al., 2021). This is due to a nonlinear photochemical process known as the Ozone-NO_x-VOC sensitivity. Volatile organic compounds or VOCs, and NO_2 are both precursors to O_3. In the VOC-limited areas where NO_x concentrations are high, increasing NO_x will lead to decreased O_3 and decreasing NO_2 would instead increase O_3. This also sheds light on the difficulty to treat NO_2 and O_3 pollution at the same time in major cities as the VOC-limited region is typical of polluted urban areas.

Table 10: Excess mortality by species after lockdown (death per million people per day)

Species	Obs	Est	Diff
$PM_{2.5}$	2.25	2.48	-0.13
PM_{10}	5.00	5.03	-0.03
SO_2	1.20	1.40	-0.19
NO_2	8.23	9.03	-0.80
CO	4.46	5.03	-0.57
O_3	8.28	8.24	0.03

Table 11: Excess mortality by regions after lockdown (death per million people per day)

Region	Obs	Est	Diff
NE	31.84	32.39	-0.55
NW	29.99	30.76	-0.77
SE	27.31	28.53	-1.22
SW	26.76	28.00	-1.24
S	19.37	21.40	-2.04
E	36.49	38.92	-2.43
C	34.27	36.81	-2.54
N	29.33	32.03	-2.70

Table 12: Total amount of Ox before and after lockdown (μg/m³)

Status	NO_2	O_3	O_x
Dur-Obs	29.25	92.27	121.52
Dur-Est	45.57	83.04	128.61
Aft-Obs	35.26	99.15	134.41
Aft-Obs	39.08	99.44	138.52

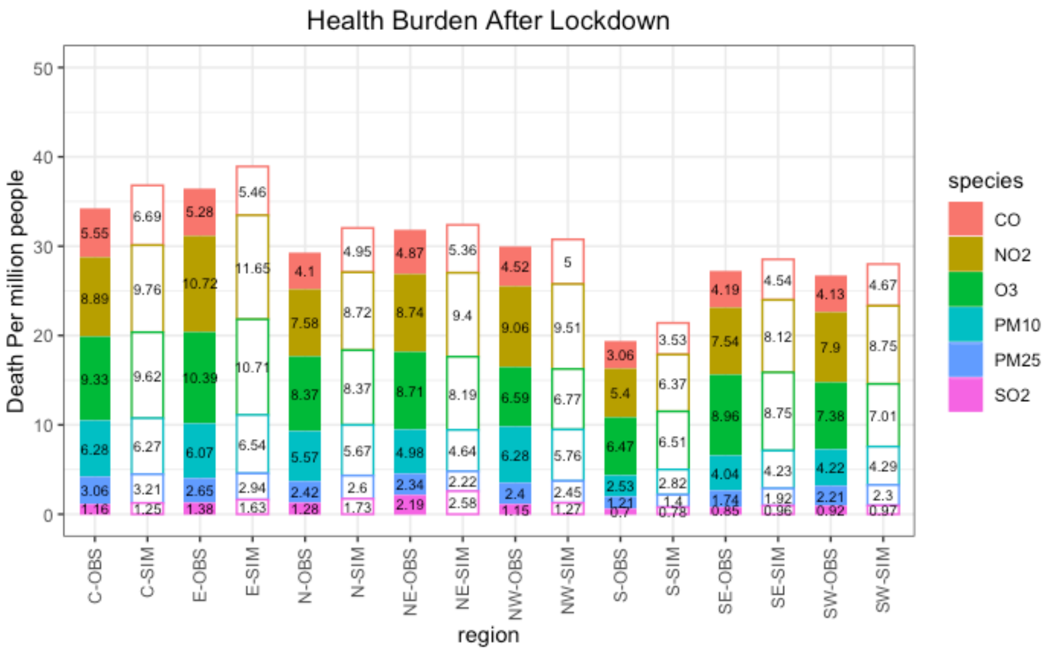

Figure 7. Observed excess mortality per species (death per million people) in 2020 after lockdown period compared against those in a counterfactual simulation without COVID-19.

3.3.2 Health economic losses

Similar to the health burden distribution, the areas where O_3 was the primary health concern (C, N, S, SE) were also places where O_3 was a primary economic concern. SO_2 is the pollutant causing the least economic losses (15.64) for all regions. The health economic losses due to the exposure to SO_2, NO_2, CO were lower during COVID for all regions. Among all species, the observation- counterfactual differences are still greatest for NO_2. To be specific, the difference between OBS-Sim results before lockdown for $PM_{2.5}$, PM_{10}, SO_2, NO_2, CO, and O_3 were -0.98, -2.8, -0.71, -6.53, -2.39, and 1.35 during the lockdown and -0.24, -0.13, -0.32, -1.37, -0.92, and 0.03 after lockdown, respectively. In modeled result, E (Primarily owing to O_3 and NO_2) has the greatest health economic losses due to air pollution (85.45). S has the lowest combined mortality (37.12). In actual observation, the ranking of combined mortality per region is consistent with machine learning output, which also corroborates the validity of the model.

Table 13: Health Economic Losses by species after lockdown (million yuan per million people per day)

Species	Obs	Est	Diff
$PM_{2.5}$	3.74	3.98	-0.24
PM_{10}	8.32	8.45	-0.13
SO_2	1.96	2.28	-0.32
NO_2	13.80	15.17	-1.37
CO	7.65	8.57	-0.92
O_3	13.55	13.52	0.03

Table 14: Health Economic Losses by regions after lockdown (million yuan per million people per day)

Region	Obs	Est	Diff
NE	41.71	42.43	-0.72
NW	39.77	40.79	-1.02
SW	37.30	39.02	-1.72
SE	54.62	57.08	-2.46
S	33.55	37.12	-3.57
C	51.68	55.50	-3.82
N	53.43	58.39	-4.96
E	80.07	85.45	-5.39

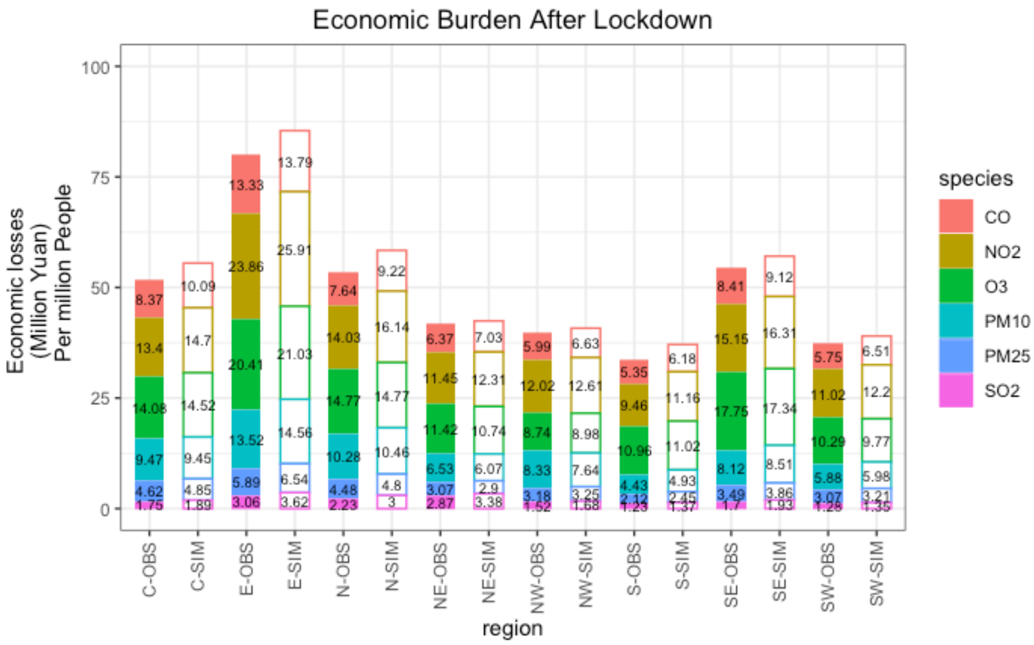

Figure 8. Observed health economic losses per species (million yuan per million people) in 2020 after the lockdown period compared against those in a counterfactual simulation without COVID-19.

3.4 Limitation & Strengths

Data availability and quality has been major issues. For many of the demographic data (e.g., baseline mortality) the national statistical yearbook only had the data for each province, instead of for each individual city. Therefore, we could only use provincial data as proxies in calculations. For those data that had to be at the city level, (e.g., city population), the national statistical yearbook only had the values available for provincial capitals. For non-capital cities, we needed to rely on alternative sources, such as the statistical yearbook of each province, which unfortunately usually does not match those from the national stat yearbook. We were not able to contrast the excess deaths due to COVID-19 vs the lives saved due to improved air quality conditions as we couldn't find data for COVID-related deaths in China in each city.

Data availability also played a role in our mortality and economic loss analysis. Unfortunately, we were not able to conduct an age-stratified health analysis, as we failed to find relevant literature that included response coefficients by age group for all six species. For the consistency of our analysis, we only calculated all-age mortality. The multi-species cumulative health impact was also an important factor to consider for a more comprehensive health analysis but we lacked information to do so.

Despite the limitations, the study also has its strength. The study is highly interdisciplinary and combines data from natural science and social science, and estimated the atmospheric, health, and economic impact of COVID-19 on air quality. It is also one of the first papers to analyze the long-term post lockdown air quality and uses ensemble machine learning algorithms XGBoost. Unlike standalone machine learning algorithms, such as decision trees and random forests, ensemble learning combines the output from multiple models and further optimizes the performance. The high model performance created a more trustworthy counterfactual world and the large sample size also allowed to provide a comprehensive overview of air quality change in China post lockdown.

3.5 Future steps

In the future, we plan to apply more machine learning models (Support Vector Machine, Random Forest and Neural Network etc.) to the data, compare how different models perform and take the best performing part. Even though XGBoost model has already done a good job of predicting pollution concentration, we believe the ensemble of different model algorithms would do even better, as has been corroborated in earlier studies. (Di et al., 2019; Di et al., 2020; Requia et al., 2020) We also would like to extend our study period to the two years after lockdown and assess if the post-lockdown effect is still present and how that has changed in magnitude. Since two years is not a short-term, we could also conduct a sensitivity analysis with long-term exposure response coefficients and see how different the results are from the short-term coefficients. We also want to include more cities and use age-stratified exposure-response coefficients to have the estimation of excess mortality and health economic losses at a higher resolution.

4 Reference:

1. Makam P, Matsa R. "Big Three" Infectious Diseases: Tuberculosis, Malaria and HIV/AIDS. Curr Top Med Chem. 2021;21(31):2779-2799. doi: 10.2174/1568026621666210916170417. PMID: 34530712.
2. https://www.reuters.com/business/imf-sees-cost-covid-pandemic-rising-beyond-125-trillion-estimate-2022-01-20/
3. Cole MA, Elliott RJR, Liu B. The Impact of the Wuhan Covid-19 Lockdown on Air Pollution and Health: A Machine Learning and Augmented Synthetic Control Approach. Environ Resour Econ (Dordr). 2020;76(4):553-580. doi: 10.1007/s10640-020-00483-4. Epub 2020 Aug 10. PMID: 32836865; PMCID: PMC7416596.
4. Jiabao Hu, Yuepeng Pan, Yuexin He, Xiyuan Chi, Qianqian Zhang, Tao Song, Weishou Shen, Changes in air pollutants during the COVID-19 lockdown in Beijing: Insights from a machine-learning technique and implications for future control policy,Atmospheric and Oceanic Science Letters,Volume 14, Issue 4,2021,100060,ISSN 1674-2834, https://doi.org/10.1016/j.aosl.2021.100060.
5. Yunjie Wang, Yifan Wen, Yue Wang, Shaojun Zhang, K. Max Zhang, Haotian Zheng, Jia Xing, Ye Wu, and Jiming Hao, Four-Month Changes in Air Quality during and after the COVID-19 Lockdown in Six Megacities in China, Environmental Science & Technology Letters 2020 7 (11), 802-808, DOI: 10.1021/acs.estlett.0c00605

6. Dong, J., Liu, X., Zhang, B., Wang, J., Shang, K., 2016. Meta-analysis of association between short-term ozone exposure and population mortality in China. Huanjing Kexue Xuebao. 36, 1477–1485.
7. Lai, H.-K., Tsang, H., Wong, C.-M., 2013. Meta-analysis of adverse health effects due to air pollution in chinese populations. BMC Public Health 13, 360–372.
8. Shang, Y., Sun, Z., Cao, J., Wang, X., Zhong, L., Bi, X., Li, H., Liu, W., Zhu, T., Huang, W., 2013. Systematic review of chinese studies of short-term exposure to air pollution and daily mortality. Environ. Int. 54, 100–111.
9. Chen, K., Zhou, L., Chen, X., Bi, J., Kinney, P.L., 2017. Acute effect of ozone exposure on daily mortality in seven cities of Jiangsu province, China: No clear evidence for threshold. Environ. Res. 155, 235–241.
10. Yao, M., Wu, G., Zhao, X., Zhang, J., 2020. Estimating health burden and economic loss attributable to short-term exposure to multiple air pollutants in China. Environ. Res. 183, 109184–109194.
11. Rybarczyk, Y., & Zalakeviciute, R. (2021). Assessing the COVID-19 impact on air quality: A machine learning approach. Geophysical Research Letters, 48, e2020GL091202. https://doi.org/10.1029/2020GL091202
12. Mario Lovrić, Kristina Pavlović, Matej Vuković, Stuart K. Grange, Michael Haberl, Roman Kern, Understanding the true effects of the COVID-19 lockdown on air pollution by means of machine learning, Environmental

Pollution, Volume 274, 2021, 115900, ISSN 0269-7491, https://doi.org/10.1016/j.envpol.2020.115900.

13. Nie D, Shen F, Wang J, Ma X, Li Z, Ge P, Ou Y, Jiang Y, Chen M, Chen M, Wang T, Ge X. Changes of air quality and its associated health and economic burden in 31 provincial capital cities in China during COVID-19 pandemic. Atmos Res. 2021 Feb;249:105328. doi: 10.1016/j.atmosres.2020.105328. Epub 2020 Oct 20. PMID: 33100451; PMCID: PMC7574695.
14. He, G., Pan, Y. & Tanaka, T. The short-term impacts of COVID-19 lockdown on urban air pollution in China. Nat Sustain 3, 1005–1011 (2020). https://doi.org/10.1038/s41893-020-0581-y
15. Shang Y, Sun Z, Cao J, Wang X, Zhong L, Bi X, Li H, Liu W, Zhu T, Huang W. Systematic review of Chinese studies of short-term exposure to air pollution and daily mortality. Environ Int. 2013 Apr;54:100-11. doi: 10.1016/j.envint.2013.01.010. Epub 2013 Feb 19. PMID: 23434817.
16. Li M, Wang T, Xie M, Li S, Zhuang B, Fu Q, Zhao M, Wu H, Liu J, Saikawa E, Liao K. Drivers for the poor air quality conditions in North China Plain during the COVID-19 outbreak. Atmos Environ (1994). 2021 Feb 1;246:118103. doi: 10.1016/j.atmosenv.2020.118103. Epub 2020 Nov 25. PMID: 33250658; PMCID: PMC7686771.
17. Silva, R.A., West, J.J., Zhang, Y., Anenberg, S.C., Lamarque, J.-F., Shindell, D.T., Collins, W.J., Dalsoren, S., Faluvegi, G., Folberth, G., Horowitz, L.W., Nagashima, T., Naik, V., Rumbold, S., Skeie, R., Sudo, K., Takemura, T.,

Bergmann, D., Cameron- Smith, P., Cionni, I., Doherty, R.M., Eyring, V., Josse, B., MacKenzie, I.A., Plummer, D., Righi, M., Stevenson, D.S., Strode, S., Szopa, S., Zeng, G., 2013. Global premature mortality due to anthropogenic outdoor air pollution and the contribution of past climate change. Environ. Res. Lett. 8 https://doi.org/10.1088/1748-9326/8/ 3/034005.

18. Zhao, X., Yu, X., Wang, Y., Fan, C., 2016. Economic evaluation of health losses from air pollution in Beijing, China. Environ. Sci. Pollut. Res. 23, 11716–11728.
19. Hanna, S.R. (1993). Uncertainties in Air Quality Model Predictions. In: Kaplan, H., Dinar, N., Lacser, A., Alexander, Y. (eds) Transport and Diffusion in Turbulent Fields. Springer, Dordrecht. https://doi.org/10.1007/978-94-011-2749-3_1
20. Chang, J., Hanna, S. Air quality model performance evaluation. Meteorol Atmos Phys 87, 167–196 (2004). https://doi.org/10.1007/s00703-003-0070-7
21. Shi Z, Song C, Liu B, Lu G, Xu J, Van Vu T, Elliott RJR, Li W, Bloss WJ, Harrison RM. Abrupt but smaller than expected changes in surface air quality attributable to COVID-19 lockdowns. Sci Adv. 2021 Jan 13;7(3):eabd6696. doi: 10.1126/sciadv.abd6696. PMID: 33523881; PMCID: PMC7806219.
22. Li K, Jacob DJ, Liao H, Qiu Y, Shen L, Zhai S, Bates KH, Sulprizio MP, Song S, Lu X, Zhang Q, Zheng B, Zhang Y, Zhang J, Lee HC, Kuk SK. Ozone pollution in the North China Plain spreading into the late-winter haze season.

Proc Natl Acad Sci U S A. 2021 Mar 9;118(10):e2015797118. doi: 10.1073/pnas.2015797118. PMID: 33649215; PMCID: PMC7958175.

23. Chen G, Tao J, Wang J, Dong M, Li X, Sun X, Cheng S, Fan J, Ye Y, Xiao J, Hu J, He G, Sun J, Lu J, Guo L, Li X, Rong Z, Zeng W, Zhou H, Chen D, Li J, Yuan L, Bi P, Du Q, Ma W, Liu T. Reduction of air pollutants and associated mortality during and after the COVID-19 lockdown in China: Impacts and implications. Environ Res. 2021 Sep;200:111457. doi: 10.1016/j.envres.2021.111457. Epub 2021 Jun 2. PMID: 34089745; PMCID: PMC8170876.
24. Xiao Q, Geng G, Xue T, Liu S, Cai C, He K, Zhang Q. Tracking PM2.5 and O3 Pollution and the Related Health Burden in China 2013-2020. Environ Sci Technol. 2021 Dec 23. doi: 10.1021/acs.est.1c04548. Epub ahead of print. PMID: 34941243.
25. Di Q, Amini H, Shi L, Kloog I, Silvern R, Kelly J, Sabath MB, Choirat C, Koutrakis P, Lyapustin A, Wang Y, Mickley LJ, Schwartz J. An ensemble-based model of PM2.5 concentration across the contiguous United States with high spatiotemporal resolution. Environ Int. 2019 Sep;130:104909. doi: 10.1016/j.envint.2019.104909. Epub 2019 Jul 1. PMID: 31272018; PMCID: PMC7063579.
26. Di Q, Amini H, Shi L, Kloog I, Silvern R, Kelly J, Sabath MB, Choirat C, Koutrakis P, Lyapustin A, Wang Y, Mickley LJ, Schwartz J. Assessing NO2 Concentration and Model Uncertainty with High Spatiotemporal

Resolution across the Contiguous United States Using Ensemble Model Averaging. Environ Sci Technol. 2020 Feb 4;54(3):1372-1384. doi: 10.1021/acs.est.9b03358. Epub 2020 Jan 14. PMID: 31851499; PMCID: PMC7065654.

27. Requia WJ, Di Q, Silvern R, Kelly JT, Koutrakis P, Mickley LJ, Sulprizio MP, Amini H, Shi L, Schwartz J. An Ensemble Learning Approach for Estimating High Spatiotemporal Resolution of Ground-Level Ozone in the Contiguous United States. Environ Sci Technol. 2020 Sep 15;54(18):11037-11047. doi: 10.1021/acs.est.0c01791. Epub 2020 Sep 1. PMID: 32808786; PMCID: PMC7498146.

28.

5 Appendix

Graph:

1. AQ predicted vs observed Per city (PM25) –boxplot

   Cities name with * refers to statistically significant Wilcoxon test result

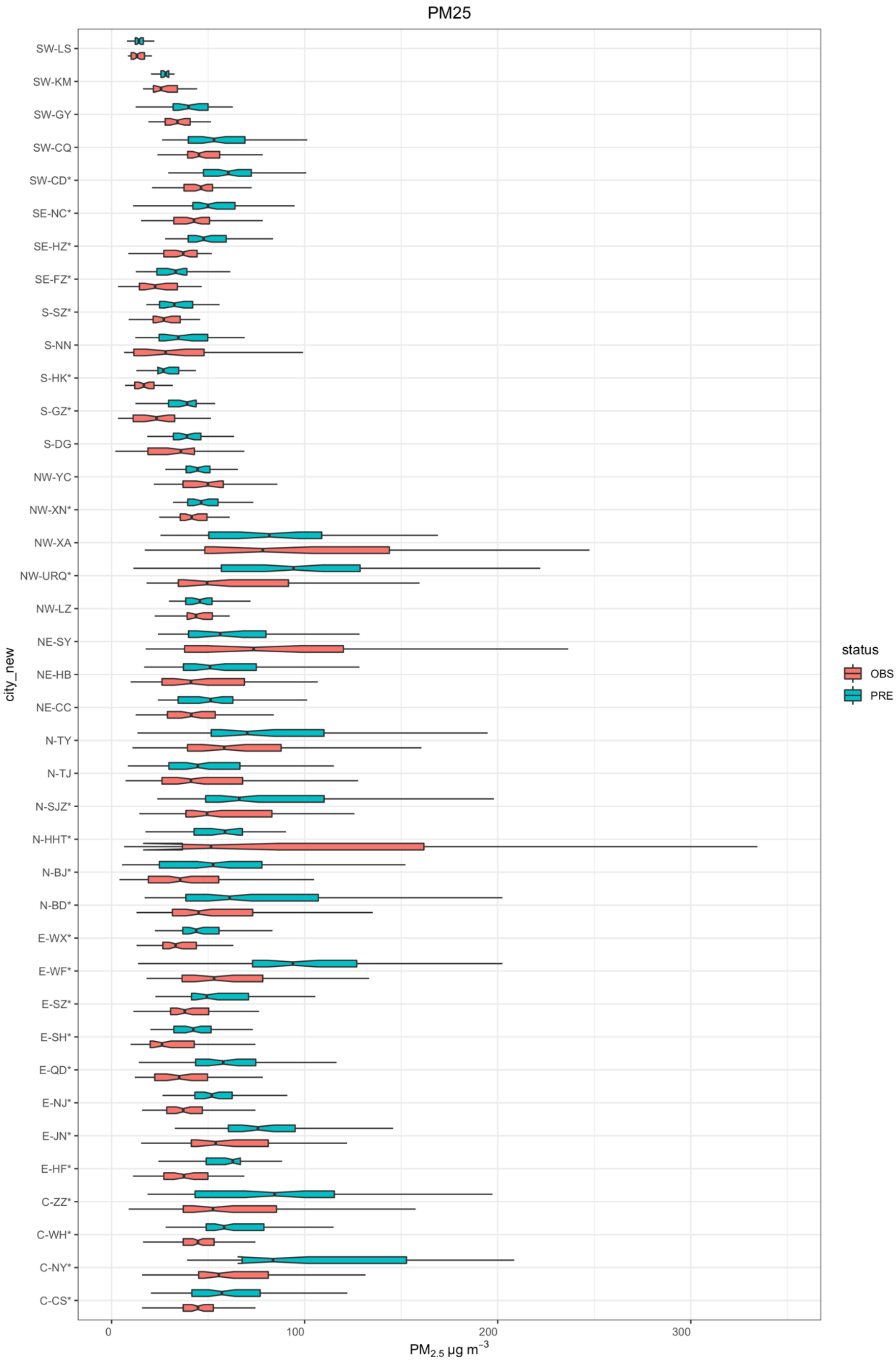

PM25
SW-LS
SW-KM
SW-GY
SW-CQ
SW-CD*
SE-NC*
SE-HZ*
SE-FZ*
S-SZ*
S-NN
S-HK*
S-GZ*
S-DG
NW-YC
NW-XN*
NW-XA
NW-URQ*
NW-LZ
NE-SY
NE-HB
NE-CC
N-TY
N-TJ
N-SJZ*
N-HHT*
N-BJ*
N-BD*
E-WX*
E-WF*
E-SZ*
E-SH*
E-QD*
E-NJ*
E-JN*
E-HF*
C-ZZ*
C-WH*
C-NY*
C-CS*
city_new
0
100
200
300
PM2.5 μg m-3
status
OBS
PRE

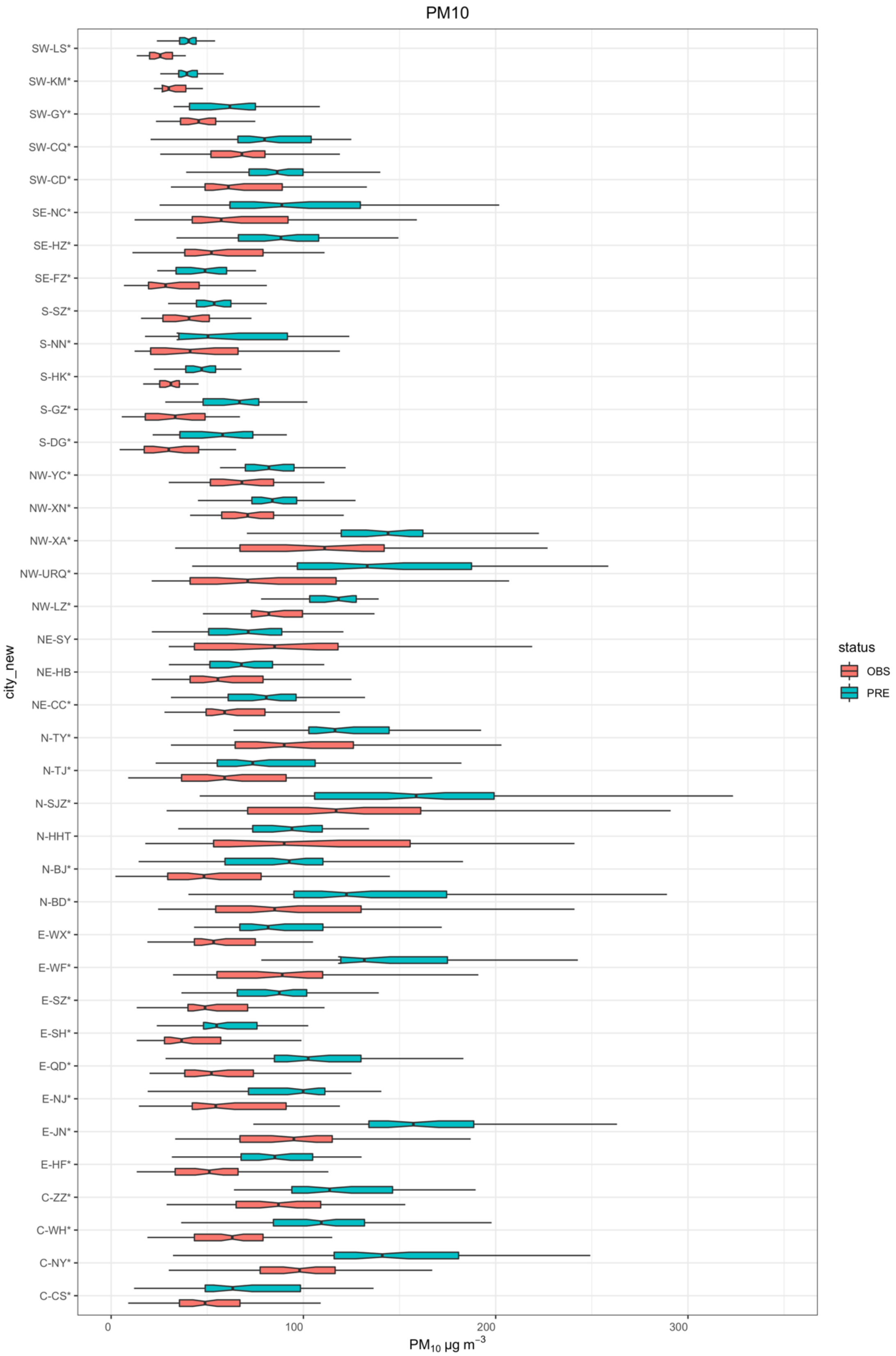
PM10
SW-LS*
SW-KM*
SW-GY*
SW-CQ*
SW-CD*
SE-NC*
SE-HZ*
SE-FZ*
S-SZ*
S-NN*
S-HK*
S-GZ*
S-DG*
NW-YC*
NW-XN*
NW-XA*
NW-URQ*
NW-LZ*
NE-SY
NE-HB
NE-CC*
N-TY*
N-TJ*
N-SJZ*
N-HHT
N-BJ*
N-BD*
E-WX*
E-WF*
E-SZ*
E-SH*
E-QD*
E-NJ*
E-JN*
E-HF*
C-ZZ*
C-WH*
C-NY*
C-CS*
city_new
0
100
200
300
PM_{10} μg m^{-3}
status
OBS
PRE

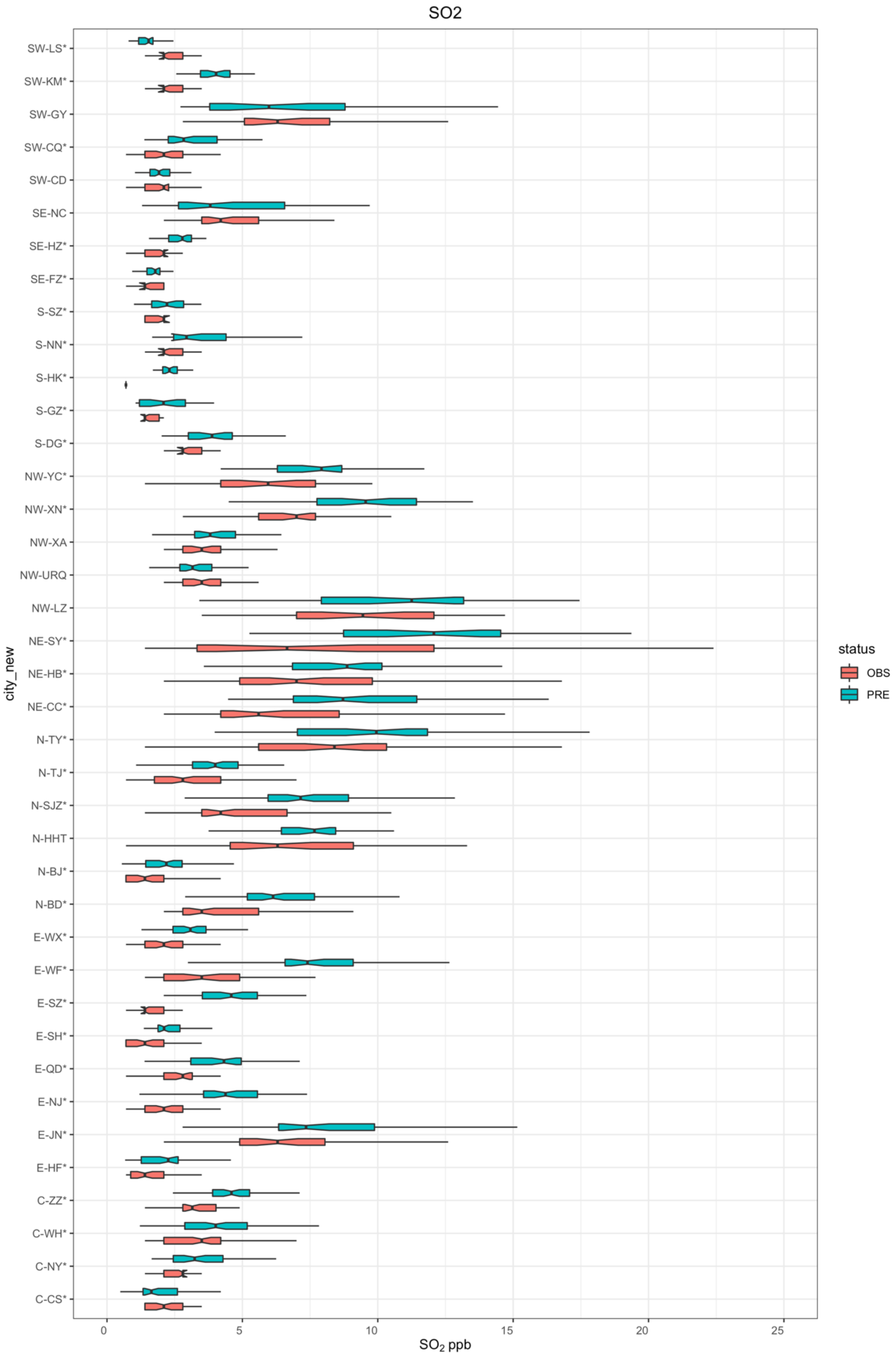
SO2
SW-LS*
SW-KM*
SW-GY
SW-CQ*
SW-CD
SE-NC
SE-HZ*
SE-FZ*
S-SZ*
S-NN*
S-HK*
S-GZ*
S-DG*
NW-YC*
NW-XN*
NW-XA
NW-URQ
NW-LZ
NE-SY*
NE-HB*
NE-CC*
N-TY*
N-TJ*
N-SJZ*
N-HHT
N-BJ*
N-BD*
E-WX*
E-WF*
E-SZ*
E-SH*
E-QD*
E-NJ*
E-JN*
E-HF*
C-ZZ*
C-WH*
C-NY*
C-CS*
city_new
0
5
10
15
20
25
SO_2 ppb
status
OBS
PRE

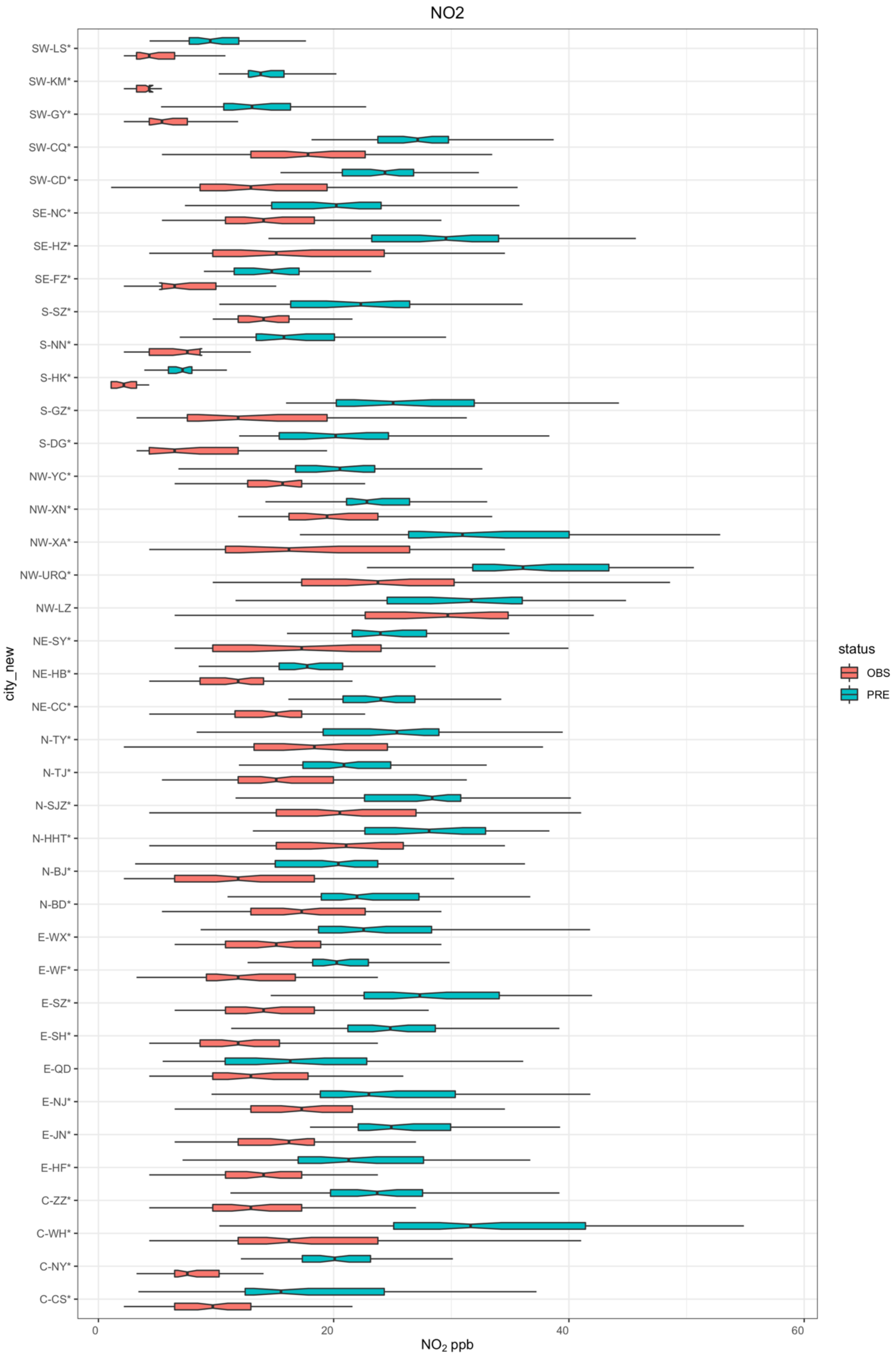
NO2
SW-LS*
SW-KM*
SW-GY*
SW-CQ*
SW-CD*
SE-NC*
SE-HZ*
SE-FZ*
S-SZ*
S-NN*
S-HK*
S-GZ*
S-DG*
NW-YC*
NW-XN*
NW-XA*
NW-URQ*
NW-LZ
NE-SY*
NE-HB*
NE-CC*
N-TY*
N-TJ*
N-SJZ*
N-HHT*
N-BJ*
N-BD*
E-WX*
E-WF*
E-SZ*
E-SH*
E-QD
E-NJ*
E-JN*
E-HF*
C-ZZ*
C-WH*
C-NY*
C-CS*
city_new
0
20
40
60
NO2 ppb
status
OBS
PRE

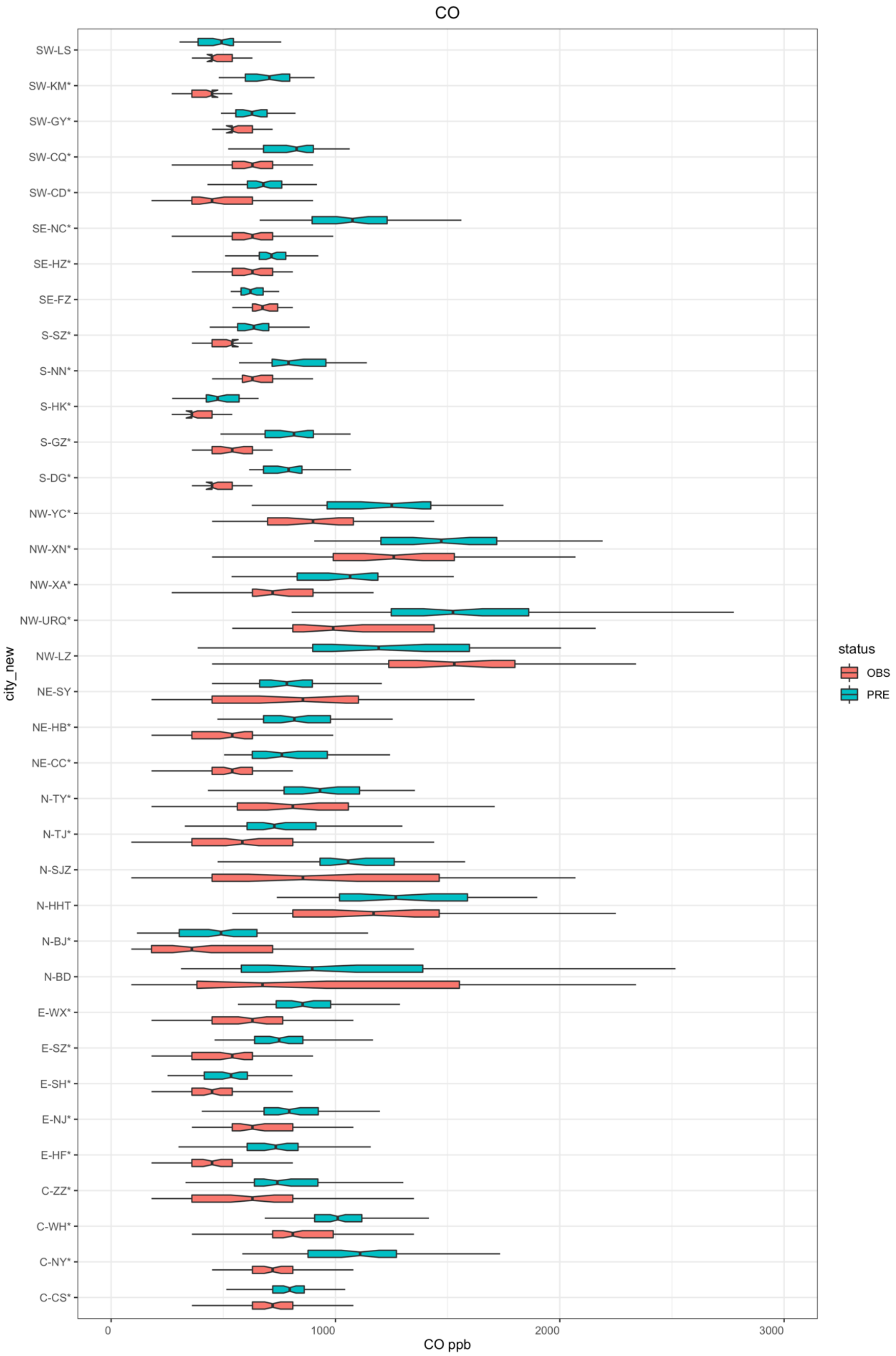
CO
SW-LS
SW-KM*
SW-GY*
SW-CQ*
SW-CD*
SE-NC*
SE-HZ*
SE-FZ
S-SZ*
S-NN*
S-HK*
S-GZ*
S-DG*
NW-YC*
NW-XN*
NW-XA*
NW-URQ*
NW-LZ
NE-SY
NE-HB*
NE-CC*
N-TY*
N-TJ*
N-SJZ
N-HHT
N-BJ*
N-BD
E-WX*
E-SZ*
E-SH*
E-NJ*
E-HF*
C-ZZ*
C-WH*
C-NY*
C-CS*
city_new
0
1000
2000
3000
CO ppb
status
OBS
PRE

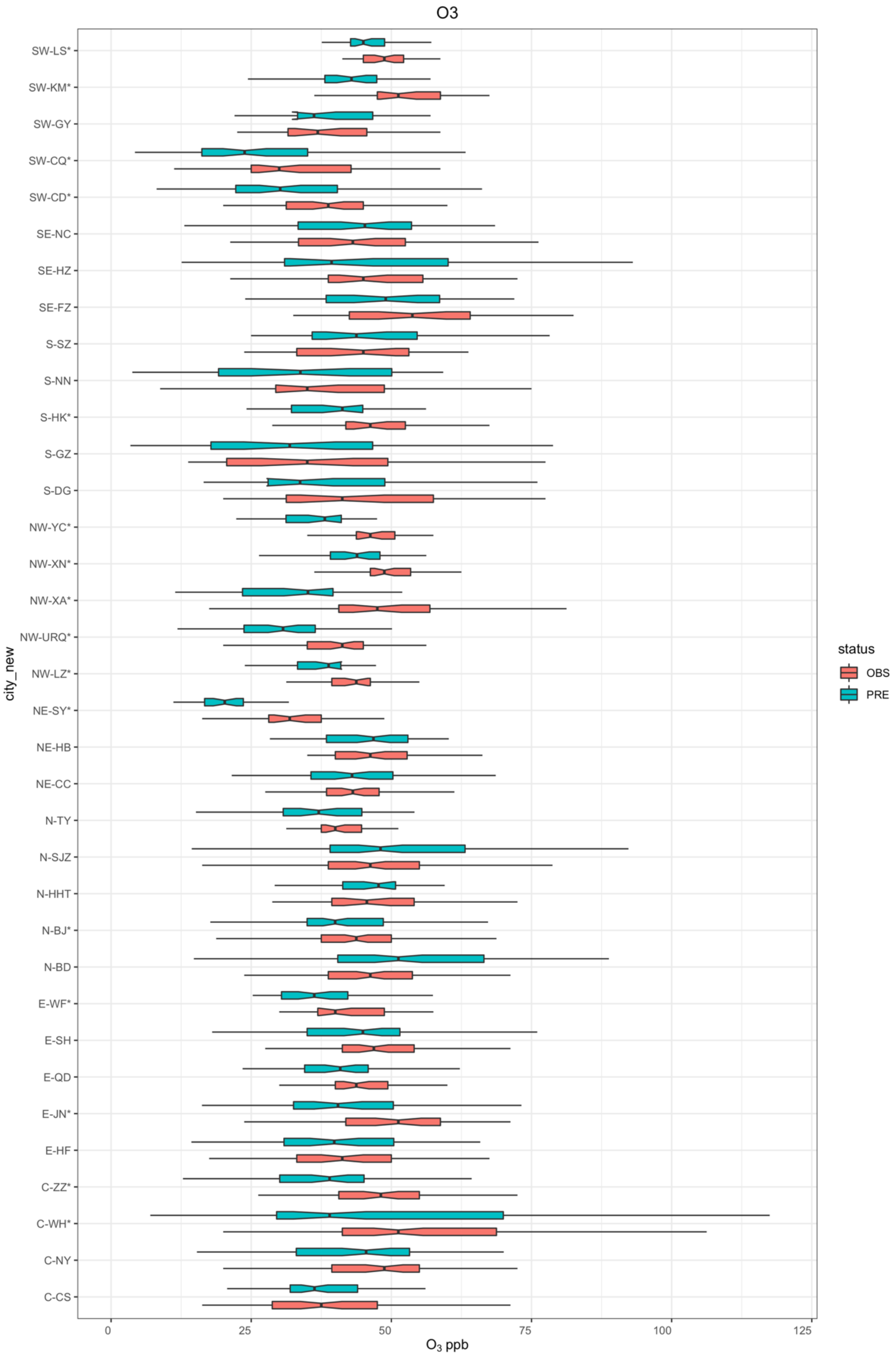

2. Health Analysis Per city

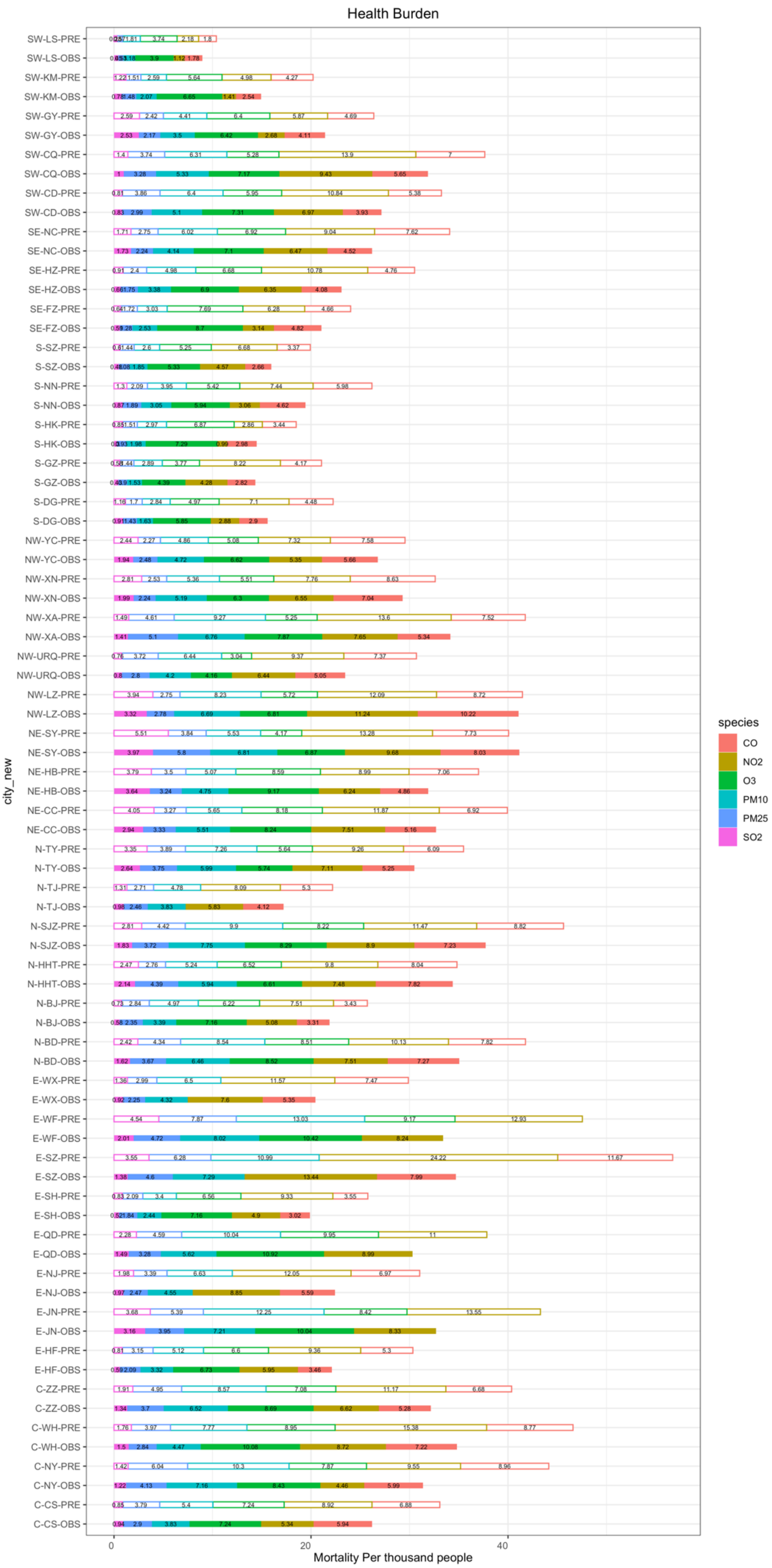
Health Burden
SW-LS-PRE
SW-LS-OBS
SW-KM-PRE
SW-KM-OBS
SW-GY-PRE
SW-GY-OBS
SW-CQ-PRE
SW-CQ-OBS
SW-CD-PRE
SW-CD-OBS
SE-NC-PRE
SE-NC-OBS
SE-HZ-PRE
SE-HZ-OBS
SE-FZ-PRE
SE-FZ-OBS
S-SZ-PRE
S-SZ-OBS
S-NN-PRE
S-NN-OBS
S-HK-PRE
S-HK-OBS
S-GZ-PRE
S-GZ-OBS
S-DG-PRE
S-DG-OBS
NW-YC-PRE
NW-YC-OBS
NW-XN-PRE
NW-XN-OBS
NW-XA-PRE
NW-XA-OBS
NW-URQ-PRE
NW-URQ-OBS
NW-LZ-PRE
NW-LZ-OBS
NE-SY-PRE
NE-SY-OBS
NE-HB-PRE
NE-HB-OBS
NE-CC-PRE
NE-CC-OBS
N-TY-PRE
N-TY-OBS
N-TJ-PRE
N-TJ-OBS
N-SJZ-PRE
N-SJZ-OBS
N-HHT-PRE
N-HHT-OBS
N-BJ-PRE
N-BJ-OBS
N-BD-PRE
N-BD-OBS
E-WX-PRE
E-WX-OBS
E-WF-PRE
E-WF-OBS
E-SZ-PRE
E-SZ-OBS
E-SH-PRE
E-SH-OBS
E-QD-PRE
E-QD-OBS
E-NJ-PRE
E-NJ-OBS
E-JN-PRE
E-JN-OBS
E-HF-PRE
E-HF-OBS
C-ZZ-PRE
C-ZZ-OBS
C-WH-PRE
C-WH-OBS
C-NY-PRE
C-NY-OBS
C-CS-PRE
C-CS-OBS
city_new
0
20
40
Mortality Per thousand people
species
CO
NO2
O3
PM10
PM25
SO2

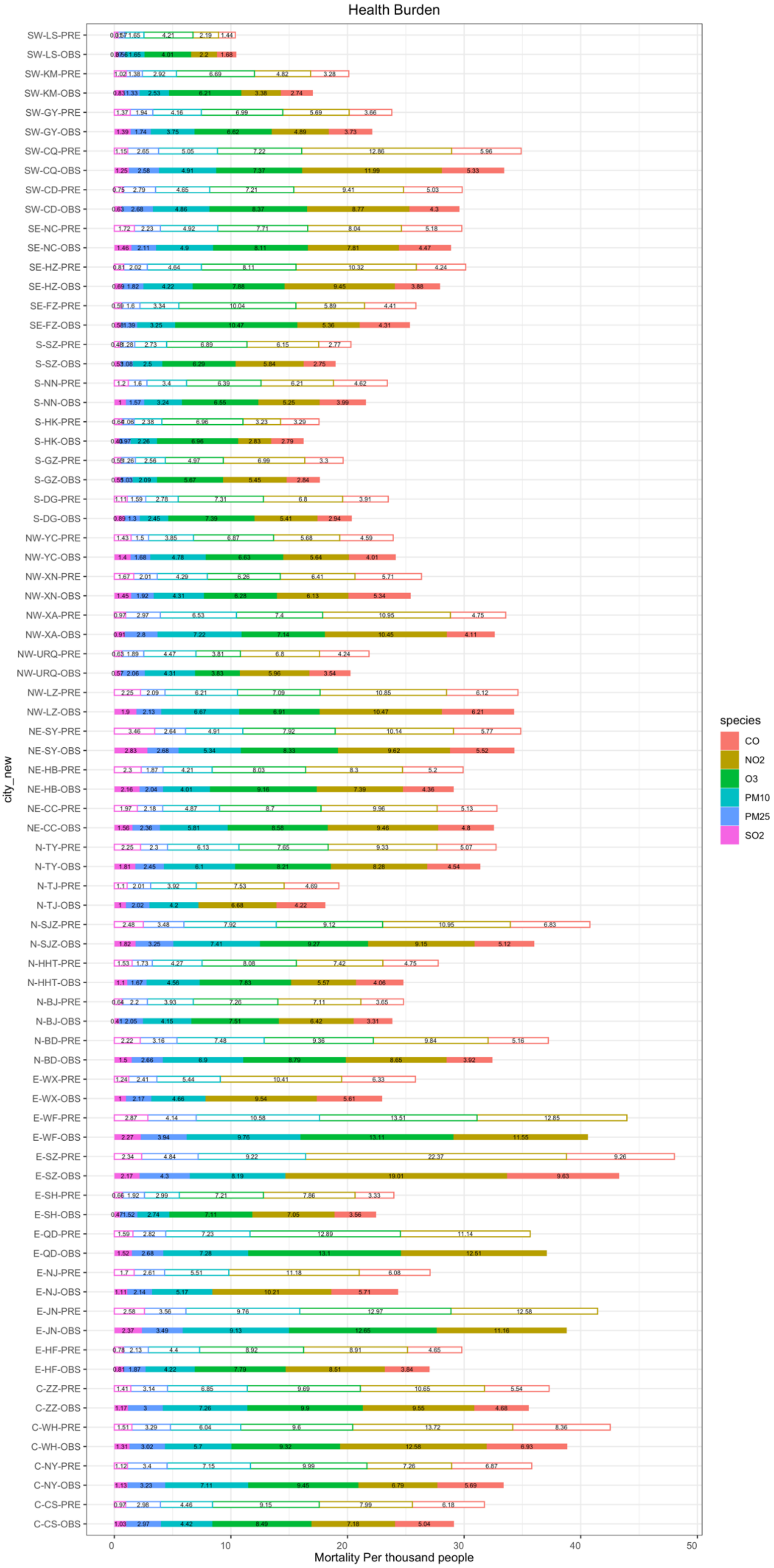
Health Burden
city_new
Mortality Per thousand people
species
CO
NO2
O3
PM10
PM25
SO2

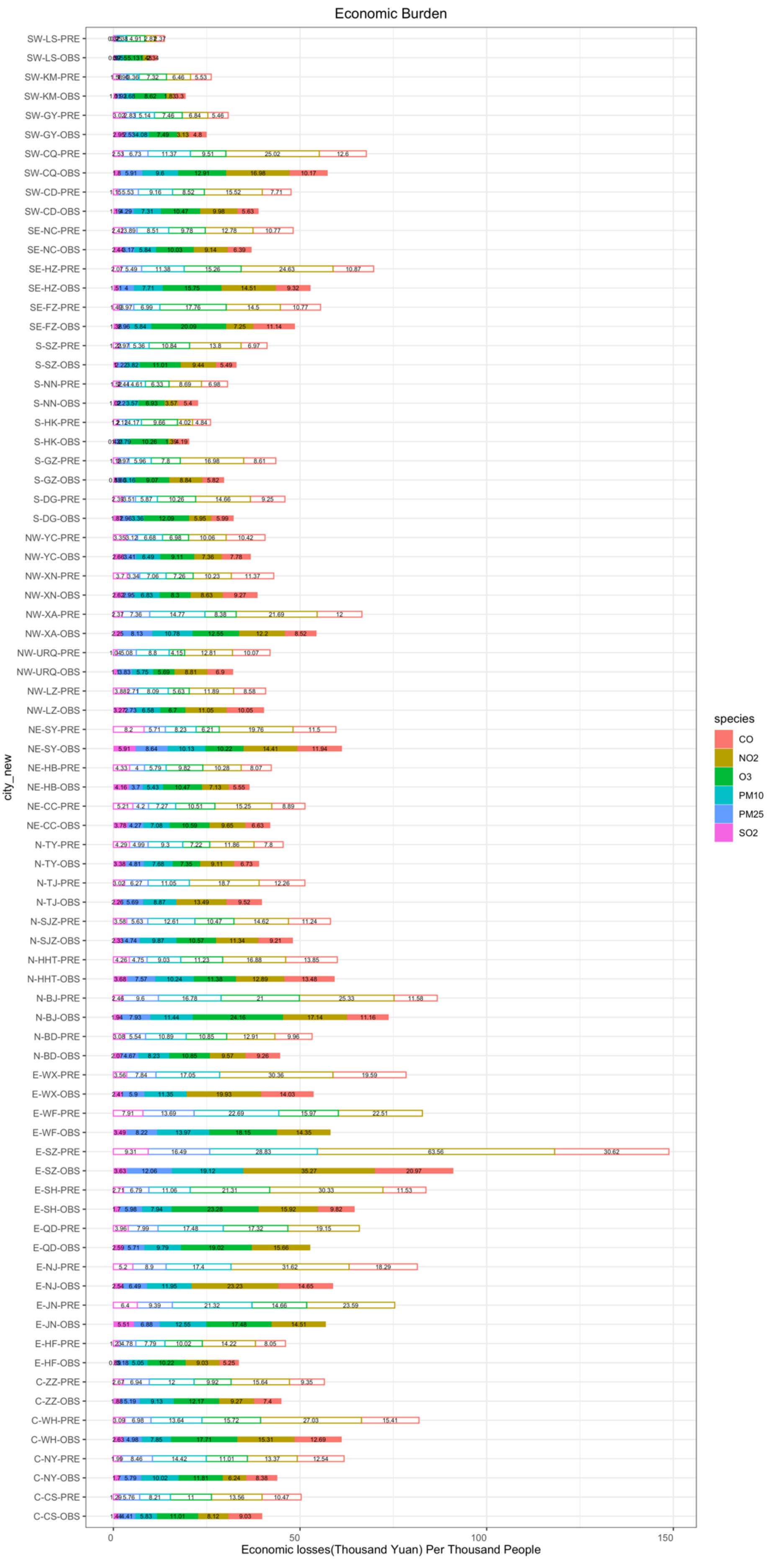
Economic Burden
species
CO
NO2
O3
PM10
PM25
SO2
city_new
Economic losses(Thousand Yuan) Per Thousand People

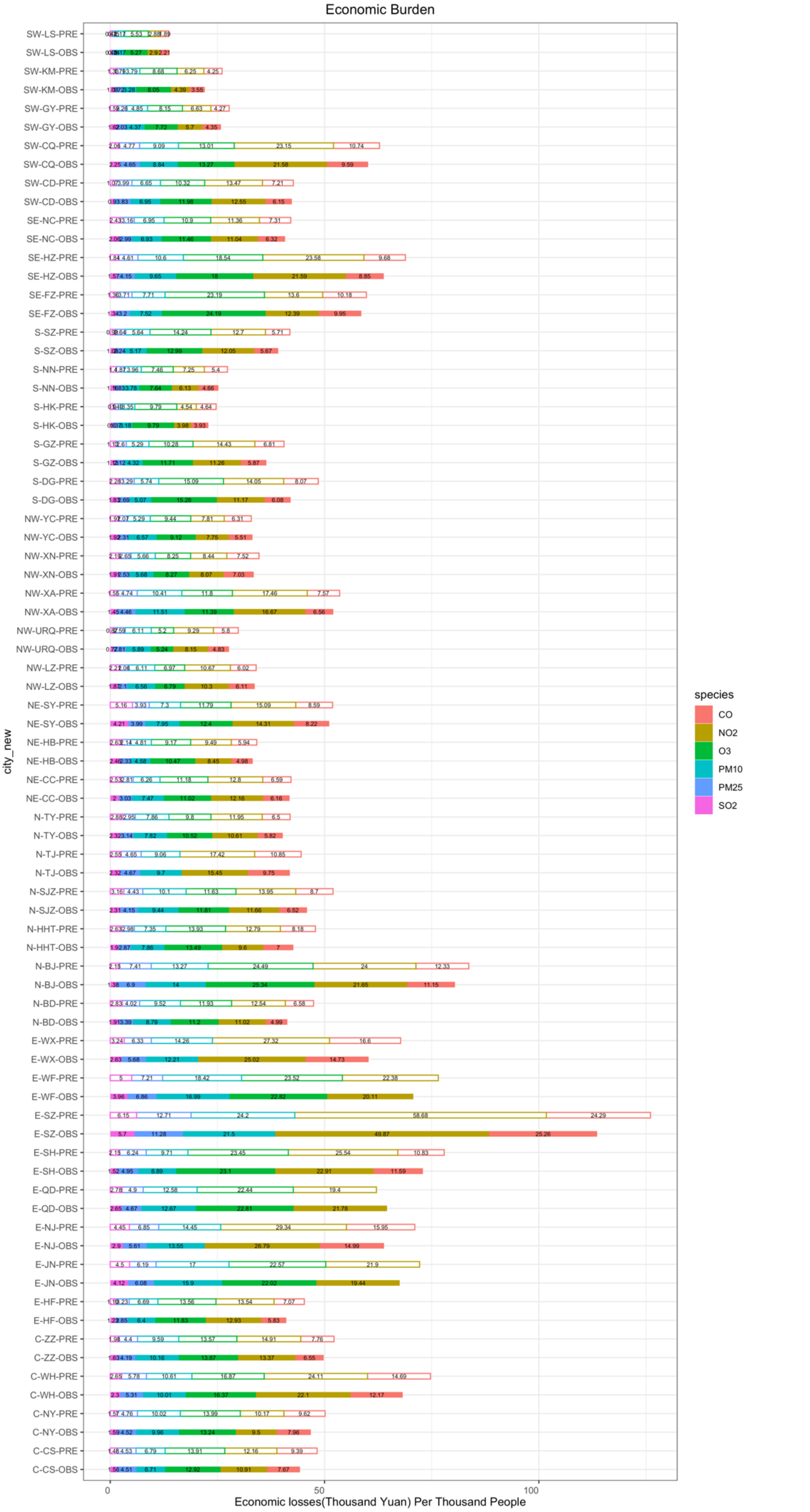
Economic Burden
city_new
Economic losses(Thousand Yuan) Per Thousand People
species
CO
NO2
O3
PM10
PM25
SO2